AGU PUBLICATIONS

Geophysical Research Letters

RESEARCH LETTER
10.1002/2017GL072909

Key Points:
- Regolith dust that can be electrostatically transported carries unusually large negative charges
- The observed negative charge polarity is contrary to the generally expected positive charges on regolith dust emitting photoelectrons
- It provides critical initial charge state for dust dynamics studies to understand the surface evolution of airless bodies

Correspondence to:
X. Wang,
xu.wang@colorado.edu

Citation:
Schwan, J., X. Wang, H.-W. Hsu, E. Grün, and M. Horányi (2017), The charge state of electrostatically transported dust on regolith surfaces, *Geophys. Res. Lett.*, *44*, 3059–3065, doi:10.1002/2017GL072909.

Received 1 FEB 2017
Accepted 30 MAR 2017
Accepted article online 3 APR 2017
Published online 14 APR 2017

The charge state of electrostatically transported dust on regolith surfaces

J. Schwan[1,2], X. Wang[1,2], H.-W. Hsu[1,2], E. Grün[1,2], and M. Horányi[1,2]

[1]Laboratory for Atmospheric and Space Physics, University of Colorado Boulder, Boulder, Colorado, USA, [2]Institute for Modeling Plasma Atmospheres and Cosmic Dust, NASA/SSERVI, Boulder, Colorado, USA

Abstract The charge state of dust particles on regolith surfaces exposed to ultraviolet radiation or plasma is investigated for understanding the role of electrostatic dust transport in the surface evolution of airless planetary bodies. Our charge measurement shows that the regolith dust that can be electrostatically transported or lofted carries large negative charges. This result is consistent with our "patched charge model," which predicts that dust particles forming microcavities in the regolith surfaces can attain large negative charges by collecting photoelectrons and/or secondary electrons emitted from neighboring particles and the resulting repulsive forces between these negatively charged particles lead to their mobilization. The observed negative charge polarity is contrary to the generally expected positive charges on the regolith dust emitting photoelectrons. The measured negative charges are orders of magnitude larger than the prediction by classical charging models. Our laboratory measurements provide critical initial charging conditions for regolith dust dynamics studies.

1. Introduction

The charging, mobilization, and subsequent transport of dust particles on airless planetary bodies due to exposure to solar wind plasma and/or solar ultraviolet (UV) radiation is an important physical process in shaping their surfaces. Electrostatic processes can change the morphology and porosity of the surface and thus its thermal inertia [*Vernazza et al.,* 2012]. Surface materials with different compositions can be relocated by dust migration [*Lee*, 1996]. More importantly, dust mobilization may alter the space weathering processes on the regolith surfaces due to the change of its surface exposure to the solar wind and may affect remote sensing spectral measurements and the albedo due to its size resorting [*Garrick-Bethell et al.,* 2011; *Pieters and Noble*, 2016].

Electrostatic dust transport has been suggested to be responsible for several unexplained space observations. The so-called "lunar horizon glow" observed five decades ago during the Apollo missions [*Criswell*, 1973; *Rennilson and Criswell*, 1974; *Colwell et al.,* 2007], the intermittently appearing radial spokes in the rings of Saturn [*Smith et al.,* 1981, 1982; *Mitchell et al.,* 2006], the fine dust deposits or "dust ponds" accumulating in craters on asteroid Eros [*Robinson et al.,* 2001; *Hughes et al.,* 2008] and comet 67P [*Thomas et al.,* 2015], the unexpectedly smooth surface of Saturn's icy moon Atlas [*Hirata and Miyamoto*, 2012], and the high surface porosity of asteroids [*Vernazza et al.,* 2012] are all examples where electrostatic dust transport may participate in surface processes. In addition, dust charging and transport is also an outstanding question for laboratory plasmas. Dust particles can accumulate and grow on the walls of fusion devices [*Pigarov et al.,* 2005] or on semiconductor wafers [*Selwyn et al.,* 1989] due to plasma-surface interactions. These particles (nanometers to micrometers in diameter) may be ejected off the surface and transported, causing contamination of the core fusion plasma or damage to the wafer.

A number of dedicated laboratory experiments have demonstrated that dust particles can indeed be mobilized and lofted from surfaces exposed to various plasma environments [*Sheridan et al.,* 1992; *Flanagan and Goree*, 2006; *Wang et al.,* 2009, 2010, 2011]. Prior experimental work has also demonstrated the significance of cohesion between dust particles in dust lofting [*Hartzell et al.,* 2013]. Theoretical models have been developed for understanding the charging of dust particles resting on a surface [*Flanagan and Goree*, 2006; *Sheridan and Hayes*, 2011; *Heijmans and Nijdam*, 2016], which differs from the charging process of an isolated (suspended) dust particle immersed in a plasma [*Shukla and Eliasson*, 2009].

Many studies including theoretical works and computer simulations have been performed to follow the dynamics of charged dust on the surfaces of airless bodies [e.g., *Nitter et al.,* 1998; *Colwell et al.,* 2005;

Poppe et al., 2012; *Hartzell and Scheeres*, 2013; *Nordheim et al.,* 2015]. However, as of yet, there is a lack of knowledge regarding the initial charge state of regolith dust, which is a critical input parameter for modeling studies.

In previous charging models (reviewed in *Wang et al*. [2016b]), a dust particle on a surface, either smooth or dusty, has been classically treated as a part of the surface because in most practical applications the Debye length is much larger than the radius of the particle. However, these classical charging models could not predict large enough charges and/or electric fields for dust particles to become mobilized and lofted under either laboratory or space conditions. The charge of dust particles resting on a smooth conducting surface with various surface biases in a plasma has been measured using a Faraday cup in the laboratory [*Wang et al.,* 2007]. The average charge of dust particles on a dusty surface in plasma was estimated from the surface potential measurement with an electrostatic voltmeter [*Ding et al.,* 2013]. None of these charge measurements showed sufficiently large charges for dust mobilization either.

Understanding of the electrostatic dust transport problem has been recently advanced with our new patched charge model, developed through our new laboratory experiments [*Wang et al*., 2016b]. This model recognizes that a dusty surface has a unique characteristic that differentiates it from a smooth surface, which is the formation of microcavities within the surface by neighboring dust particles. In most situations, dust particles resting on a surface with more than one layer can be treated as a dusty surface. The existence of microcavities changes the charging process of a dusty surface to be a volume effect, in which charges can be stored within the microcavities. We briefly summarize the principles of our new patched charge model and its predictions.

2. Predictions of the Patched Charge Model

In this patched charge model [*Wang et al*., 2016b], UV photons and/or plasma electrons and ions can reach dust particles below the surface through the small openings between dust particles on the top layer, creating photoelectrons and/or secondary electrons inside the microcavities underneath. A large fraction of these emitted electrons will be absorbed on the surfaces of the dust particles comprising the boundaries of the microcavities. This generates a negative charge Q_r on the surface patches within microcavities, in addition to a charge Q_b on the particles' top surface patches that are directly exposed to plasma or UV. It was shown that $|Q_r| \gg |Q_b|$ and the resulting repulsive forces between these negative charges are suggested to be responsible for dust mobilization and transport.

The electric field at the top surface patch E_b is the sheath electric field that is inversely proportional to the Debye length λ_{De}. The electric field within the microcavity E_r is the Coulomb electric field that is inversely proportional to the characteristic dimension of the microcavity, which is approximated to be the radius, a, of the particles. In most laboratory and space conditions, $\lambda_{De} \gg a$, so $E_r \gg E_b$, and consequently, $|Q_r| \gg |Q_b|$. The net charge Q can thus be approximated to be Q_r for a spherical particle,

$$Q \approx Q_r \approx -0.5C(\eta T_{ee}/e) \tag{1}$$

where $C = 4\pi\varepsilon_0 a$ is the capacitance of an isolated spherical particle, T_{ee} is the emitted electron temperature in eV, and η is a factor larger than 1, to account for the enhanced surface potential due to the collection of high-energy electrons in the tail of the emitted electron energy distribution. The term $\eta T_{ee}/e$ is an approximation of the potential on the collecting surface patch with respect to the emitting surface patch within the microcavity. An empirical constant for η is between 4 and 10, based on our potential measurements using a double probe [*Wang et al*., 2016b]. The factor of 0.5 is attributed to the assumption that the surface area of a microcavity surface patch is a half of the total surface area.

This new charging model makes two surprising predictions: (1) Dust particles on a dusty surface that emits photoelectrons and/or secondary electrons can attain net negative charges. This is contrary to the expected positive charge on dust particles that emit photoelectrons. And (2) the magnitude of these negative charges can be much larger than the charges predicted from previous charging models. The unusually large charges were also shown with a recent computer simulation work [*Zimmerman et al.,* 2016]. Below we present the new charge measurement results that verify both of these predictions of the patched charge model.

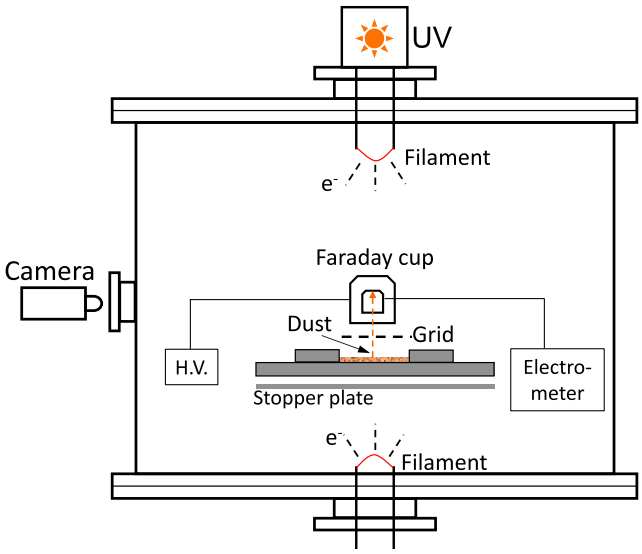

Figure 1. Schematic diagram of the experimental setup. A UV source (172 nm wavelength) on the top of the chamber illuminates the dusty surface. A top hot filament emits beam electrons (120 eV) to the surface to create secondary electrons. When the chamber is filled with argon gas, a plasma is created by impact ionization of the beam electrons. Alternatively, the bottom hot filament is used to create a thermal plasma only condition as the emitted beam electrons (40 eV for ionizing the argon gas) are prevented by a stopper plate from entering the bulk plasma above the surface. H.V. Stands for high voltage.

3. Charge Measurement and Results

Different from previous charge measurements [*Wang et al.*, 2007; *Ding et al.*, 2013], the charges of individual dust particles on dusty surfaces were directly measured in this experiment. The experiment was carried out in a vacuum chamber, 50 cm in diameter and 28 cm tall, with a base pressure of 10^{-6} torr (Figure 1). Dust particles were loaded into a crater 1.9 cm in diameter and 0.2 cm deep on a grounded graphite surface. Two types of insulating particles were used: irregular-shaped Mars simulants 38–45 μm in diameter and silica microspheres 42.3 ± 1.1 μm in diameter. As in our previous experiment [*Wang et al.*, 2016b], dust particles were charged by exposure to three different conditions: (a) thermal plasma and electron beam, (b) electron beam, and (c) UV radiation. In all three conditions, secondary electrons or photoelectrons were created by the electron beam or the UV photons. The charge measurements were then performed right after turning off the charging source, while the charge on the dust particles is expected to remain approximately unchanged in vacuum conditions. To measure the charge polarity, we applied voltages up to ±3 kV to a gridded electrode 5 mm above the dusty surface to attract −/+ charged particles from the surface and record them using a video camera. The magnitudes of the charges were measured with a Faraday cup.

Before exposure to any of the three charging conditions, we verified that no notable background charges existed, due to tribocharging, for example, as we found no dust particles being attracted from the surface while applying ±3 kV external voltages to the gridded electrode. The results remained the same for dust particles after exposure to a thermal plasma only condition in which no secondary electrons should be created due to the cold electron temperature ~ 2 eV [*Wang et al.*, 2016b]. This indicates that the charges on the dust particles in the thermal plasma were too small to allow them to be lifted off the surface, consistent with previous experimental results [*Wang et al.*, 2016b].

3.1. Charge Polarity Measurement

The charge polarity of both types of particles was examined under all three charging conditions. Using any of the charging sources, no dust particles were detached from the surface when a negative voltage was applied (up to −3 kV). In contrast, when a positive voltage was applied (around +0.5 kV), a large flux of dust particles was recorded to be accelerated through the gridded electrode, as shown in Figure 2. The one exception was that no microspheres were lofted by the external electric fields after exposure to the UV radiation. This measurement showed that a fraction of dust particles on dusty surfaces were charged with significant amount of net negative charges in all three charging conditions, even under the UV radiation. These charge results were contrary to generally expected positive charges on dust particles that emit photoelectrons while were in agreement with the predictions of our patched charge model.

3.2. Charge Magnitude Measurement

The magnitudes of charges on the dust particles were measured using a Faraday cup apparatus that consists of an inner cup coaxially embedded in an outer cup (Figure 1). A voltage of ±3 kV was applied to the outer cup

Figure 2. An example of the charge polarity measurements. The silica microspheres after exposure to an electron beam are electrostatically lofted with negative charges. The same negative polarity results are measured for both the Mars simulants and silica microspheres in all three conditions: plasma and electron beam, electron beam, and UV radiation.

in order to accelerate −/+ charged dust particles from the surface to enter through a small hole (1 mm in diameter) into the inner cup where their image charges were measured with an electrometer. The gridded electrode was now grounded and used as a gate to control when dust particles are accelerated into the Faraday cup. Before the outer cup acceleration voltage was set to the desired value, the gridded electrode was positioned between the cup and dusty surface so that there was no electric field to accelerate dust particles. Once the acceleration voltage was ready, the gridded electrode was moved out of the way to allow charged dust particles to be accelerated into the Faraday cup. This measurement procedure was performed in order to avoid false signals due to voltage variations in the electrometer induced by changing the outer cup voltage. No positive charges were observed with the Faraday cup, consistent with the charge polarity measurement results.

Figure 3 shows histograms of the negative charges measured in all three conditions for both types of particles. The measured charge distributions of both types of dust particles are broad, even for the microspheres with uniform size and shape distributions (in the range of 42.3 ± 1.1 μm in diameter). Based on our previous dust transport experiment [*Wang et al*., 2016b], dust particles accelerated into the Faraday cup are expected to have broad size distributions, which will result in broad distributions of charge as it is proportional to the diameter of dust particles. As shown in the previous experiment [*Wang et al*., 2016b], even though the initial dust sample in the crater was sieved to include particles only in the range of 38–45 μm in diameter, the lofted particles were observed to be composed of single-sized particles (38–45 μm), small residues (< 38 μm) adhered to the single-sized particles due to the dust production processes and large aggregates (up to 140 μm) as a result of the efficient clumping of single particles due to cohesion. The sizes of the electrostatically lofted Mars simulants had distributions of 20.3 ± 13.1 μm (under the UV radiation) and 44.9 ± 30.1 μm (under the electron beam) in diameter. Similar aggregation is also expected to occur for silica microspheres, leading to the formation of larger particulates with a broad size distribution. These aggregates can form complex microcavities with variable shapes and sizes. The cohesive force can vary over several orders of magnitude, depending on how dust particles contact each other [*Cooper et al.,* 2001]. One possible scenario could be that the cohesive forces between the aggregates are smaller than the repulsive forces between them while the cohesive forces between the single particles are large enough to hold them together, resulting in the lofted aggregates instead of single particles.

Additionally, the charges on approximately equal-sized single particles can also have large variations due to the variations in shape and size of the microcavities in which highly varied electric fields on the surfaces of the surrounding particles are created. It is also noted that the charge distributions for the silica microspheres are even broader than those for the Mars simulants. One possible explanation could be that the average sizes and size variations for the aggregates formed by the microspheres (42 μm in diameter) are larger than those formed by the simulants (which were composed of the single particles 45 μm in diameter and smaller residues). The exact mechanisms remain unclear.

No silica microspheres were registered in the Faraday cup after exposure to the UV radiation. It is also shown in Figure 3 that more Mars simulants were measured by the Faraday cup than the silica microspheres in the

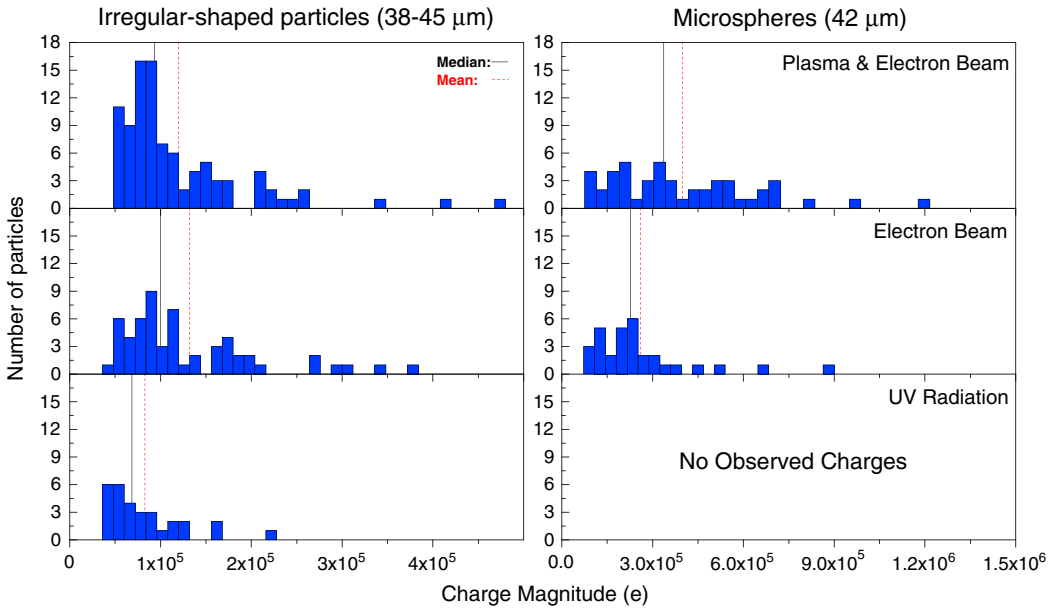

Figure 3. Histograms of the magnitudes of the negative charges measured after dust particles are exposed to: (a) plasma and electron beam, (b) electron beam, and (c) UV radiation conditions. Charge magnitude is in the unit of elementary charge *e*. To ensure consistency each histogram consists of data from 12 identical trials in each of the listed conditions.

plasma and electron beam and electron beam conditions. The difference in the number of particles being measured could be due to a difference in the cohesive forces between the silica and Mars simulant particles that have different compositions and shapes, and/or the different geometry of the characteristic microcavities formed by microspheres or irregular-shaped particles.

The average magnitudes of the measured negative charges are compared with their predicted values from the patched charge model (Figure 4). In equation (1) for the estimation of the charge magnitudes, η is 8.3, 7.3, and 4 for the UV, electron beam, and plasma and electron beam conditions [*Wang et al.*, 2016b]. T_{ee} is approximately 0.3 eV for photoelectrons [*Wang et al.,* 2008] and 3 eV for secondary electrons [*Wang et al.*, 2016a]. For the irregular-shaped Mars simulants, the particle radius *a* in equation (1) is 20.3 ± 13.1 μm (UV radiation) and 44.9 ± 30.1 μm (electron beam and plasma and electron beam) in diameter, given from the size distributions of the lofted particles measured from previous experiment [*Wang et al.*, 2016b]. For the silica microspheres, *a* is the radius of a single microsphere, 21.2 ± 0.6 μm.

The predicted charge magnitudes for the assumption of spherical particles show agreement with the measured charges of the irregular-shaped simulants, except for the UV radiation condition in which the predicted value is below the measurement threshold (dashed line). The measured charges in this condition may indicate the subset of charges larger than the threshold in the broad charge distribution as explained above. The measured charges ($> 10^5$ *e*, Figure 4) for any of the three charging conditions are 2 orders of magnitude larger than the charges ($< 1.4 \times 10^3$ *e*) predicted using previous charging models [*Wang et al.*, 2016b] or the charges ($\sim 6.3 \times 10^2$ *e*) measured from previous experimental work [*Ding et al.,* 2013]. According to the force estimations with the similar charge magnitudes [*Wang et al.*, 2016b], the repulsive forces between these largely negatively charged dust particles can indeed be responsible for their lofting and transport.

As measured from previous experiment in the electron beam condition [*Wang et al.*, 2016b], the average size of electrostatically lofted Mars simulants (mass density 1.9 g/cm^3) was 44.9 μm in diameter, corresponding to the average mass 9×10^{-11} kg. The charge-to-mass ratio (*Q*/*m*) was estimated to be 3×10^{-4} C/kg, close to the lower limit found from previous dust lofting measurement [*Wang et al.*, 2016b].

Figure 4 shows that the measured charges of the microspheres are larger than the predicted values for the single microspheres. This may be caused by the formation of large aggregates and/or the charge variability on the single particles due to the variations in shape and size of the microcavities as described above.

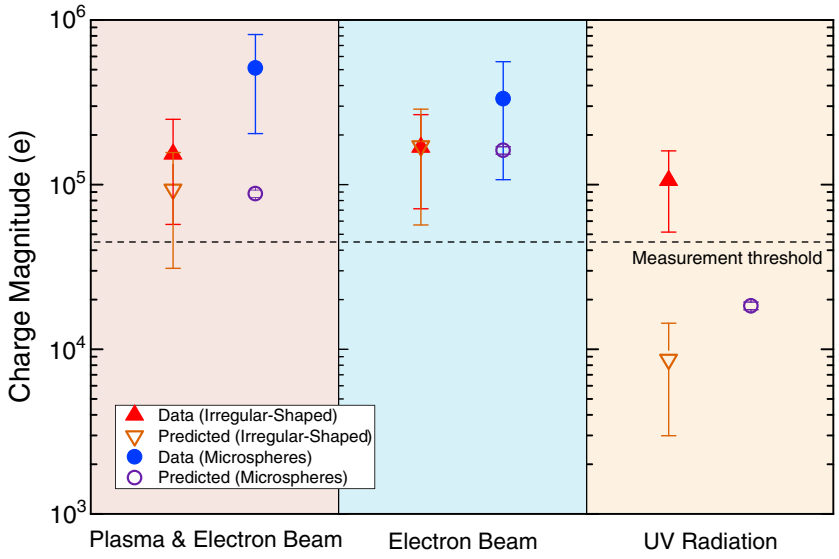

Figure 4. Mean magnitudes with standard deviations of the measured negative charges shown in Figure 3 and their predicted values from the patched charge model (equation (1)) under all three charging conditions. The parameters of η, T_{ee}, and a in equation (1) are described in section 3.2. The dashed line is the charge measurement threshold.

Our charge measurement results, including the negative charge polarity and unusually large magnitudes, are expected to be true for any shape and composition of insulating dust particles on dusty surfaces that emit photoelectrons and/or secondary electrons, according to the patched charge model. The charge magnitude may vary for different types of dust particles, depending on their photoemission and/or secondary emission yields.

4. Conclusions

Our charge measurements confirmed the predictions of the patched charge model, showing that dust particles can be electrostatically transported or lofted on the surfaces of airless planetary bodies due to their large net negative charges. This result especially contradicts the generally expected positive charge polarity on dust particles exposed to UV radiation. These negative charges are orders of magnitude larger than the charges predicted by previous charging models or measured from previous experimental works. The initial charge state of regolith dust provided from this new charge measurement is critical for their dynamics studies in order to understand the surface evolution of airless planetary bodies.

Acknowledgments
This work was supported by the NASA/SSERVI's Institute for Modeling Plasma, Atmospheres and Cosmic Dust (IMPACT). Partial support is also acknowledged by the contract JPL-1502225 at the University of Colorado from Rosetta, which is an ESA mission with contributions from its member states and NASA. This work was partially inspired by discussions at the International Space Science Institute, Bern, Switzerland within the International Team 336: "Plasma Surface Interactions with Airless Bodies in Space and Laboratory". The experimental data for this paper are available on request (contact person: Xu Wang; e-mail:xu.wang@colorado.edu).

References

Colwell, J. E., A. A. S. Gulbis, M. Horányi, and S. Robertson (2005), Dust transport in photoelectron layers and the formation of dust ponds on Eros, *Icarus*, *175*, 159–169.
Colwell, J. E., S. Batiste, M. Horányi, S. Robertson, and S. Sture (2007), Lunar surface: Dust dynamics and regolith mechanics, *Rev. Geophys.*, *45*, RG2006, doi:10.1029/2005RG000184.
Cooper, K., A. Gupta, and S. Beaudoin (2001), Simulation of the adhesion of particles to surfaces, *J. Colloid Interface Sci.*, *234*, 284–292.
Criswell, D. R. (1973), Horizon-glow and the motion of lunar dust, in *Photon and Particle Interactions With Surfaces in Space*, edited by R. J. L. Grard, pp. 545–556, Springer, New York.
Ding, N., J. Wang, and J. Polansky (2013), Measurement of dust charging on a lunar regolith simulant surface, *IEEE Trans. Plasma Sci.*, *41*, 3498–3504.
Flanagan, T. M., and J. Goree (2006), Dust release from surfaces exposed to plasma, *Phys. Plasmas*, *13*, 123,504, doi:10.1063/1.2401155.
Garrick-Bethell, I., J. W. Head III, and C. M. Pieters (2011), Spectral properties, magnetic fields, and dust transport at lunar swirls, *Icarus*, *212*, 480–492.
Hartzell, C. M., and D. J. Scheeres (2013), Dynamics of levitating dust particles near asteroids and the Moon, *J. Geophys. Res. Planets*, *118*, 116–125, doi:10.1029/2012JE004162.
Hartzell, C. M., X. Wang, D. J. Scheeres, and M. Horányi (2013), Experimental demonstration of the role of cohesion in electrostatic dust lofting, *Geophys. Res. Lett.*, *40*, 1038–1042, doi:10.1002/grl.50230.
Heijmans, L. C. J., and S. Nijdam (2016), Dust on a surface in a plasma: A charge simulation, *Phys. Plasmas*, *23*, 043703.
Hirata, N., and H. Miyamoto (2012), Dust levitation as a major resurfacing process on the surface of a Saturnian icy satellite, Atlas, *Icarus*, *220*, 106–113.
Hughes, A. L. H., J. E. Colwell, and A. W. Dewolfe (2008), Electrostatic dust transport on Eros: 3-D simulations of pond formation, *Icarus*, *195*, 630–648.

Lee, P. (1996), Dust levitation on asteroids, *Icarus*, *124*, 181–194.
Mitchell, C. J., M. Horányi, O. Havnes, and C. C. Porco (2006), Saturn's spokes: Lost and found, *Science*, *311*, 1587–1589.
Nitter, T., O. Havnes, and F. Melandsø (1998), Levitation and dynamics of charged dust in the photoelectron sheath above surfaces in space, *J. Geophys. Res.*, *103*, 6605–6620.
Nordheim, T. A., G. H. Jones, J. S. Halekas, E. Roussos, and A. J. Coates (2015), Surface charging and electrostatic dust acceleration at the nucleus of comet 67P during periods of low activity, *Planet. Space Sci.*, *119*, 24–35.
Pieters, C. M., and S. K. Noble (2016), Space weathering on airless bodies, *J. Geophys. Res. Planets*, *121*, 1865–1884, doi:10.1002/2016JE005128.
Pigarov, A. Y., S. I. Krasheninnikov, T. K. Soboleva, and T. D. Rognlien (2005), Dust-particle transport in tokamak edge plasmas, *Phys. Plasmas*, *12*, 122,508.
Poppe, A. R., M. Piquette, A. Likhanskii, and M. Horányi (2012), The effect of surface topography on the lunar photoelectron sheath and electrostatic dust transport, *Icarus*, *221*, 135–146.
Rennilson, J. J., and D. R. Criswell (1974), Surveyor observations of lunar horizon-glow, *Moon*, *10*, 121–142.
Robinson, M. S., P. C. Thomas, J. Veverka, S. Murchie, and B. Carcich (2001), The nature of ponded deposits on Eros, *Nature*, *413*, 396–400.
Selwyn, G. S., J. Singh, and R. S. Bennett (1989), In-situ laser diagnostic studies of plasma-generated particulate contamination, *J. Vac. Sci. Technol., A*, *7*, 2758–2765.
Sheridan, T. E., J. Goree, Y. T. Chiu, R. L. Rairden, and J. A. Kiessling (1992), Observation of dust shedding from material bodies in a plasma, *J. Geophys. Res.*, *97*, 2935–2942, doi:10.1029/91JA02801.
Sheridan, T. E., and A. Hayes (2011), Charge fluctuations for particles on a surface exposed to plasma, *Appl. Phys. Lett.*, *98*, 091501, doi:10.1063/1.3560302.
Shukla, P. K., and B. Eliasson (2009), Colloquium: Fundamentals of dust-plasma interactions, *Rev. Mod. Phys.*, *81*, 25–44.
Smith, B. A., et al. (1981), Encounter with Saturn-Voyager-1 imaging science results, *Science*, *212*, 163–191.
Smith, B. A., et al. (1982), A new look at the Saturn system—The Voyager 2 images, *Science*, *215*, 504–537.
Thomas, N., et al. (2015), Redistribution of particles across the nucleus of comet 67P/Churyumov-Gerasimenko, *Astron. Astrophys.*, *583*, A17, doi:10.1051/0004-6361/201526049.
Vernazza, P., et al. (2012), High surface porosity as the origin of emissivity features in asteroid spectra, *Icarus*, *221*, 1162–1172.
Wang, X., J. Colwell, M. Horányi, and S. Robertson (2007), Charge of dust on surfaces in plasma, *IEEE Trans. Plasma Sci.*, *35*, 271–279.
Wang, X., M. Horányi, and S. Robertson (2008), Plasma probes for the lunar surface, *J. Geophys. Res.*, *113*, A08108, doi:10.1029/2008JA013187.
Wang, X., M. Horányi, and S. Robertson (2009), Experiments on dust transport in plasma to investigate the origin of the lunar horizon glow, *J. Geophys. Res.*, *114*, A05103, doi:10.1029/2008JA013983.
Wang, X., M. Horányi, and S. Robertson (2010), Investigation of dust transport on the lunar surface in a laboratory plasma with an electron beam, *J. Geophys. Res.*, *115*, A11102, doi:10.1029/2010JA015465.
Wang, X., M. Horányi, and S. Robertson (2011), Dust transport near electron beam impact and shadow boundaries, *Planet. Space Sci.*, *59*, 1791–1794.
Wang, X., J. Pilewskie, H.-W. Hsu, and M. Horányi (2016a), Plasma potential in the sheaths of electron-emitting surfaces in space, *Geophys. Res. Lett.*, *43*, 525–531, doi:10.1002/2015GL067175.
Wang, X., J. Schwan, H.-W. Hsu, E. Grün, and M. Horányi (2016b), Dust charging and transport on airless planetary bodies, *Geophys. Res. Lett.*, *43*, 6103–6110, doi:10.1002/2016GL069491.
Zimmerman, M. I., W. M. Farrell, C. M. Hartzell, X. Wang, M. Horanyi, D. M. Hurley, and K. Hibbitts (2016), Grain-scale supercharging and breakdown on airless regoliths, *J. Geophys. Res. Planets*, *121*, 2150–2165, doi:10.1002/2016JE005049.